



# Scattering of evanescent waves by a particle on or near a plane surface

A. Doicu<sup>a,\*</sup>, Yu. Eremin<sup>b</sup>, T. Wriedt<sup>a</sup>

<sup>a</sup> *Institut für Werkstofftechnik, Badgasteiner Straße 3, 28359 Bremen, Germany*

<sup>b</sup> *Department of Applied Mathematics and Computer Science, Moscow State University, Vorobyov Hills, 119899 Moscow, Russia*

Received 14 April 2000; accepted 13 June 2000

---

## Abstract

The paper is devoted to semi-analytical approaches for analyzing the evanescent wave scattering by penetrable scatterers on a plane surface. On the basis of the discrete sources method and the T-matrix method numerical schemes were developed and implemented in computer programs. Numerical results related to the influence of the plane surface on the scattering characteristics are discussed. © 2001 Elsevier Science B.V. All rights reserved.

---

## 1. Introduction

The recent development in scanning near-field optical microscopy [1] has yielded spatial resolution in the 1-nm range [2], i.e. far beyond the diffraction limit of conventional optical microscopes. This limit was attained by using evanescent waves originating from a dielectric surface by total internal reflection illumination. The wide field of application of such a scattering microscopy, as for instance the Photon Scanning Tunneling Microscopy [3], gives rise to renewed interest in the numerical analysis of scattering of evanescent waves by small penetrable scatterers near the surface of a dielectric prism [4–7]. As it was pointed out by several authors, the effect of the plane surface on the differential scattering cross section is considerable. In fact the presence of the surface leads to a strong redistribution of the scattered intensity of an isolated particle [7]. In this context, the elaboration of exact models for evanescent wave scattering appears to be justified.

The paper is organized as follows. In Sections 1 and 2 we briefly present the theory of evanescent wave scattering in the context of the discrete sources method and the T-matrix method. In Section 3 we investigate from a computational point of view the elaborated methods. We also compare these models with approximate models, which does not take into account the scatterer-prism interaction. Finally, in Section 4 a summary of the results is given.

---

\* Corresponding author.

E-mail address: doicu@iwt.uni-bremen.de (A. Doicu).

## 2. Discrete sources method

The geometry of the scattering problem is shown in Fig. 1. An axisymmetric particle with a smooth boundary  $S$  and interior  $D_i$  is situated on a plane surface  $\Sigma$ , so that its symmetry axis coincides with the normal to the plane surface. The upper half-space corresponding to the ambient medium is denoted by  $D_0$ , while the lower half-space corresponding to the glass prism is denoted by  $D_1$ . Let us introduce a rectangular coordinate system  $Oxyz$  by choosing the origin  $O$  at the tangent point between the particle and the substrate. The  $z$ -axis coincides with the symmetry axis of the particle and is directed into the domain  $D_0$ . The wave number in the domain  $D_t$ ,  $t = 0, 1, i$ , is denoted by  $k_t = k\sqrt{\epsilon_t\mu_t}$ . Similarly,  $n_t$ ,  $t = 0, 1, i$ , stands for the index of refraction of the domain  $D_t$ . The external excitation  $\mathbf{E}_{\text{inc}}, \mathbf{H}_{\text{inc}}$  is a polarized plane wave propagating in the glass prism at the angle  $\beta_1$  with respect to the  $z$ -axis. If  $\beta_1 > \arcsin(n_0/n_1)$  the wave will be totally reflected and only a damped or an evanescent wave traveling along the surface will be present in the upper half-space. The mathematical formulation of the scattering problem consists in the Maxwell equations

$$\nabla \times \mathbf{E}_t = jk_t\mu_t\mathbf{H}_t \quad \nabla \times \mathbf{H}_t = -jk_t\epsilon_t\mathbf{E}_t \quad \text{in } D_t, \quad t = 0, 1, i, \quad (1)$$

the transmission conditions at the plane interface and the particle surface

$$\mathbf{e}_z \times (\mathbf{E}_1 - \mathbf{E}_0) = 0, \quad \mathbf{e}_z \times (\mathbf{H}_1 - \mathbf{H}_0) = 0 \quad \text{on } \Sigma, \quad (2)$$

and

$$\mathbf{n} \times (\mathbf{E}_i - \mathbf{E}_0) = 0, \quad \mathbf{n} \times (\mathbf{H}_i - \mathbf{H}_0) = 0 \quad \text{on } S, \quad (3)$$

respectively and the radiation (attenuation) condition at infinity. Here,  $\mathbf{n}$  is the outward unit normal vector to  $S$  and  $\mathbf{E}_t, \mathbf{H}_t$  stands for the total field in the domain  $D_t$ . Note that the total field in  $D_0$  sums the contribution of the refracted incident field and the scattered field, that is

$$\mathbf{E}_0 = \mathbf{E}_{\text{sca}} + \mathbf{E}_{\text{inc}}^{\text{ref}} \quad \text{and} \quad \mathbf{H}_0 = \mathbf{H}_{\text{sca}} + \mathbf{H}_{\text{inc}}^{\text{ref}}.$$

We will construct an approximate solution to the scattering problem by representing the electromagnetic fields as a finite linear combination of fields of multipoles [8,9]. The approximate solutions satisfy the Maxwell equations in the domains  $D_t$ ,  $t = 0, 1, i$ , the radiation condition in the domains  $D_t$ ,  $t = 0, 1$ , and the transmission condition

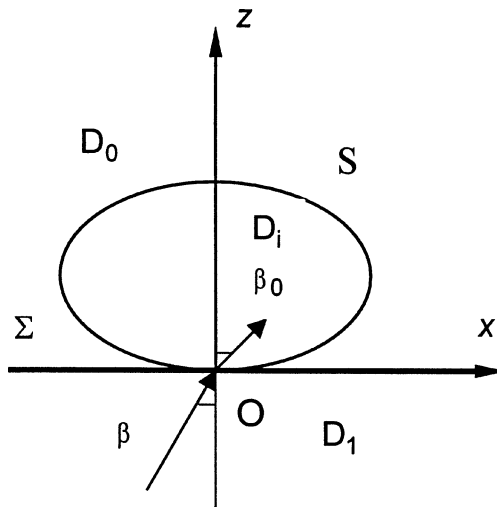


Fig. 1. Geometry of the scattering system.

at the plane interface. Essentially, the scattering problem simplifies to the approximation problem of the external excitation on the particle surface. The amplitudes of discrete sources will be determined from the transmission conditions (3).

For constructing the approximate solutions we consider the Green tensor for a stratified interface [8], that is

$$\overline{\overline{\mathbf{G}}}(\mathbf{r}, \mathbf{r}_0) = \begin{bmatrix} g^{e,h} & 0 & 0 \\ 0 & g^{e,h} & 0 \\ \frac{\partial f}{\partial x} & \frac{\partial f}{\partial y} & \sigma^{e,h} \end{bmatrix} \quad (4)$$

where the tensor elements are given by

$$g^{e,h}(\mathbf{r}, \mathbf{r}_0) = \exp(jk_0 R)/R + \int_0^\infty J_0(\lambda r) v_{11}^{e,h}(z, z_0, \lambda) \lambda \, d\lambda, \quad (5)$$

$$\sigma^{e,h}(\mathbf{r}, \mathbf{r}_0) = g^{h,e}(\mathbf{r}, \mathbf{r}_0), \quad (6)$$

and

$$f(\mathbf{r}, \mathbf{r}_0) = \int_0^\infty J_0(\lambda r) v_{31}(z, z_0, \lambda) \lambda \, d\lambda. \quad (7)$$

Here,  $r = \rho^2 + \rho_0^2 - 2\rho\rho_0 \cos(\varphi - \varphi_0)$ ,  $(\rho, \varphi, z)$  are the cylindrical coordinates of the observation point  $\mathbf{r}$ ,  $(\rho_0, \varphi_0, z_0)$  are the cylindrical coordinates of the source point  $\mathbf{r}_0$ ,  $R = [r^2 + (z - z_0)^2]^{1/2}$  and, for  $z \geq 0$  and  $z_0 > 0$ , the spectral functions  $v_{11}^{e,h}$  and  $v_{31}$  are given by

$$v_{11}^e(z, z_0, \lambda) = \frac{\mu_1 K_z^0 - \mu_0 K_z^1}{\mu_1 K_z^0 + \mu_0 K_z^1} \frac{1}{K_z^0} \exp[-K_z^0(z + z_0)], \quad (8)$$

$$v_{11}^h(z, z_0, \lambda) = \frac{\epsilon_1 K_z^0 - \epsilon_0 K_z^1}{\epsilon_1 K_z^0 + \epsilon_0 K_z^1} \frac{1}{K_z^0} \exp[-K_z^0(z + z_0)], \quad (9)$$

$$v_{31}(z, z_0, \lambda) = \frac{2(\mu_1 \epsilon_1 - \mu_0 \epsilon_0)}{(\mu_1 K_z^0 + \mu_0 K_z^1)(\epsilon_1 K_z^0 + \epsilon_0 K_z^1)} \exp[-K_z^0(z + z_0)], \quad (10)$$

where  $K_z^t = (\lambda^2 - k_t^2)^{1/2}$ ,  $t = 0, 1$ .

Let  $\{z_n\}_{n=1}^\infty$  be a dense sequence of source points distributed on a segment  $\Gamma_z$  of the axis of symmetry  $Oz$ , i.e.  $z_n \in \Gamma_z$ , where  $\Gamma_z$  is located inside  $D_i$ . For the field in the ambient medium we define the Hertz vectors of vector multipoles by

$$\mathbf{A}_{mnx}^{e,h}(\mathbf{r}) = \mathbf{e}_x g_m^{e,h}(\rho, z, z_n) - \mathbf{e}_z f_{m+1}(\rho, z, z_n) \cos \varphi, \quad (11)$$

$$\mathbf{A}_{mny}^{e,h}(\mathbf{r}) = \mathbf{e}_y g_m^{e,h}(\rho, z, z_n) - \mathbf{e}_z f_{m+1}(\rho, z, z_n) \sin \varphi,$$

and the Hertz vectors of vertical electric dipoles by

$$\mathbf{A}_{0n}^{e,0}(\mathbf{r}) = g_0^h(\rho, z, z_n) \mathbf{e}_z, \quad (12)$$

where  $g_m^{e,h}$  and  $f_m$  stands for the azimuthal harmonics of the tensor components  $g^{e,h}$  and  $f$ . For the field inside the particle we define entire functions with singularities located at infinity by

$$\mathbf{A}_{mnx}^i(\mathbf{r}) = \mathbf{e}_x Y_m^i(\rho, z, z_n), \quad \mathbf{A}_{mny}^i(\mathbf{r}) = \mathbf{e}_y Y_m^i(\rho, z, z_n) \quad (13)$$

and Hertz vectors of vertical electric dipoles by

$$\mathbf{A}_{0n}^{e,i}(\mathbf{r}) = Y_0^i(\rho, z, z_n)\mathbf{e}_z. \quad (14)$$

Here,

$$Y_m^i(\rho, z, z_0) = j_m \left[ k_i \sqrt{\rho^2 + (z - z_0)^2} \right] \left( \frac{\rho}{\sqrt{\rho^2 + (z - z_0)^2}} \right)^m \quad (15)$$

with  $j_m$  standing for the spherical Bessel function.

An approximate solution to the scattering problem will be constructed by taking into account not only the rotational symmetry of the scatter, but simultaneously the polarization of the external excitation [8,9]. In this context, for a P-polarized incident field we use some linear combinations of  $\mathbf{A}_{mnx}^{e,h}$  and  $\mathbf{A}_{mny}^{e,h}$ , that is

$$\begin{aligned} \mathbf{A}_{mn}^{e,0}(\mathbf{r}) &= \mathbf{A}_{mnx}^e(\mathbf{r}) \cos m\varphi - \mathbf{A}_{mny}^e(\mathbf{r}) \sin m\varphi, \\ \mathbf{A}_{mn}^{h,0}(\mathbf{r}) &= \mathbf{A}_{mnx}^h(\mathbf{r}) \sin m\varphi + \mathbf{A}_{mny}^h(\mathbf{r}) \cos m\varphi. \end{aligned} \quad (16)$$

In the same manner we construct the following linear combinations

$$\begin{aligned} \mathbf{A}_{mn}^{e,i}(\mathbf{r}) &= \mathbf{A}_{mnx}^i(\mathbf{r}) \cos m\varphi - \mathbf{A}_{mny}^i(\mathbf{r}) \sin m\varphi, \\ \mathbf{A}_{mn}^{h,i}(\mathbf{r}) &= \mathbf{A}_{mnx}^i(\mathbf{r}) \sin m\varphi + \mathbf{A}_{mny}^i(\mathbf{r}) \cos m\varphi \end{aligned} \quad (17)$$

to represent the fields inside the particle.

Then, after defining the elementary fields of electric and magnetic multipoles

$$\begin{pmatrix} \mathbf{E}_{mn}^{e,t}(\mathbf{r}) \\ \mathbf{H}_{mn}^{e,t}(\mathbf{r}) \end{pmatrix} = \begin{pmatrix} j/k\varepsilon_t\mu_t \nabla \times \nabla \times \mathbf{A}_{mn}^{e,t}(\mathbf{r}) \\ 1/\mu_t \nabla \times \mathbf{A}_{mn}^{e,t}(\mathbf{r}) \end{pmatrix}, \quad (18)$$

$$\begin{pmatrix} \mathbf{E}_{mn}^{h,t}(\mathbf{r}) \\ \mathbf{H}_{mn}^{h,t}(\mathbf{r}) \end{pmatrix} = \begin{pmatrix} -1/\varepsilon_t \nabla \times \mathbf{A}_{mn}^{h,t}(\mathbf{r}) \\ j/k\varepsilon_t\mu_t \nabla \times \nabla \times \mathbf{A}_{mn}^{h,t}(\mathbf{r}) \end{pmatrix} \quad (19)$$

and the elementary fields of electric dipoles

$$\begin{pmatrix} \mathbf{E}_n^{e,t}(\mathbf{r}) \\ \mathbf{H}_n^{e,t}(\mathbf{r}) \end{pmatrix} = \begin{pmatrix} j/k\varepsilon_t\mu_t \nabla \times \nabla \times \mathbf{A}_{0n}^{e,t}(\mathbf{r}) \\ 1/\mu_t \nabla \times \mathbf{A}_{0n}^{e,t}(\mathbf{r}) \end{pmatrix}, \quad (20)$$

where  $t = 0, i$ , we can represent the approximate solution of the scattering problem for  $P$  polarized field as

$$\begin{aligned} \begin{pmatrix} \mathbf{E}_t^{\mathcal{N}}(\mathbf{r}) \\ \mathbf{H}_t^{\mathcal{N}}(\mathbf{r}) \end{pmatrix} &= \sum_{n=1}^N \sum_{m=0}^M \left[ e_{mn,t}^{\mathcal{N}} \begin{pmatrix} \mathbf{E}_{mn}^{e,t}(\mathbf{r}) \\ \mathbf{H}_{mn}^{e,t}(\mathbf{r}) \end{pmatrix} + f_{mn,t}^{\mathcal{N}} \begin{pmatrix} \mathbf{E}_{mn}^{h,t}(\mathbf{r}) \\ \mathbf{H}_{mn}^{h,t}(\mathbf{r}) \end{pmatrix} \right] \\ &+ \sum_{n=1}^N r_{n,t}^{\mathcal{N}} \begin{pmatrix} \mathbf{E}_n^{e,t}(\mathbf{r}) \\ \mathbf{H}_n^{e,t}(\mathbf{r}) \end{pmatrix}. \end{aligned} \quad (21)$$

Here,  $\mathcal{N}$  is a complex index incorporating  $M$  and  $N$ . The completeness of the system of distributed multipoles guarantee the convergence of the approximate solution to the exact solution in closed subsets of  $D_0$  [8]. As mentioned before the above representations fulfilled the conditions of the scattering problem except the transmission condition at the particle surface. In fact this condition will be used to determine the amplitudes of discrete sources. Various schemes for amplitude determination are at our disposal. As it has been found stable

results can be obtained by using pseudoinversion of an over-determined system of linear equations. After the amplitudes of discrete sources have been determined one can calculate the far-field pattern  $\mathbf{E}_{s\infty}$  of the scattered field  $\mathbf{E}_s$  by using the asymptotic representation for the Sommerfeld integrals [9].

### 2.1. T-matrix method

For modeling the scattering problem in the framework of the T-matrix method we use the same notations as before but we choose the origin  $O$  at the distance  $z_0$  above the plane interface. Since, the basic formulae for Mie scattering of evanescent waves result from analytic continuation of the standard case of plane wave excitation, we represent the external excitation as a series of regular spherical vector wave functions (SVWF)  $\mathbf{M}_{mn'}^1(k_0\mathbf{r})$  and  $\mathbf{N}_{mn'}^1(k_0\mathbf{r})$ , i.e.

$$\mathbf{E}_{\text{inc}}^{\text{ref}}(\mathbf{r}) = \sum_{n'=1}^{\infty} \sum_{m=-n'}^{n'} D_{mn'} [a_{mn'}^{\text{ref}} \mathbf{M}_{mn'}^1(k_0\mathbf{r}) + b_{mn'}^{\text{ref}} \mathbf{N}_{mn'}^1(k_0\mathbf{r})]. \quad (22)$$

Here,  $D_{mn'}$  is a normalization constant and is given by

$$D_{mn'} = \frac{2n'+1}{4n'(n'+1)} \cdot \frac{(n'-|m|)!}{(n'+|m|)!}.$$

The expansion coefficients  $a_{mn'}^{\text{ref}}$  and  $b_{mn'}^{\text{ref}}$  are the coefficients of the refracted plane wave traveling in the  $(0, \beta_0)$  direction and are given by

$$\begin{aligned} a_{mn'}^{\text{ref}} &= -4j^{n'} [jm\pi_n^{|m|}(\beta_0)t_{\parallel}(\beta_1)E_{\beta_1} + \tau_n^{|m|}(\beta_0)t_{\perp}(\beta_1)E_{\alpha_1}], \\ b_{mn'}^{\text{ref}} &= -4j^{n'+1} [\tau_n^{|m|}(\beta_0)t_{\parallel}(\beta_1)E_{\beta_1} - jm\pi_n^{|m|}(\beta_0)t_{\perp}(\beta_1)E_{\alpha_1}]. \end{aligned} \quad (23)$$

In the above equation  $E_{\beta_1}$  and  $E_{\alpha_1}$  are the parallel and perpendicular component of the electric field, respectively,  $\pi_n^{|m|}(\theta) = P_n^{|m|}(\cos\theta)/\sin\theta$  and  $\tau_n^{|m|}(\theta) = dP_n^{|m|}(\cos\theta)/d\theta$ , where  $P_n^{|m|}(\cos\theta)$  are the associated Legendre polynomials, and  $t_{\parallel}$  and  $t_{\perp}$  denotes the Fresnel transmission coefficients for parallel and perpendicular polarizations, respectively. For  $\beta_1 > \beta_c = \arcsin(n_0/n_1)$ , it follows from Snell's law that  $\sin\beta_0 > 1$ , hence  $\cos\beta_0$  becomes purely imaginary. We choose  $\cos\beta_0 = j\sqrt{\sin^2\beta_0 - 1}$ , since otherwise the amplitude of the refracted wave would tend to infinity with increasing distance. Note, that the expansion (22) is also valid for complex propagation angles if the analytic continuation of the Legendre polynomials to complex values of the argument is considered.

The scattered field contains the contribution of the direct scattered field

$$\mathbf{E}_{\text{sca}}^0(\mathbf{r}) = \sum_{n=1}^{\infty} \sum_{m=-n}^n D_{mn} [e_{mn} \mathbf{M}_{mn}^3(k_0\mathbf{r}) + f_{mn} \mathbf{N}_{mn}^3(k_0\mathbf{r})] \quad (24)$$

and the reflected or the interacted field

$$\mathbf{E}_{\text{sca}}^R(\mathbf{r}) = \sum_{n=1}^{\infty} \sum_{m=-n}^n D_{mn} [e_{mn} \mathbf{M}_{mn}^{3,R}(k_0\mathbf{r}) + f_{mn} \mathbf{N}_{mn}^{3,R}(k_0\mathbf{r})], \quad (25)$$

where  $\mathbf{M}_{mn}^{3,R}(k_0\mathbf{r})$  and  $\mathbf{N}_{mn}^{3,R}(k_0\mathbf{r})$  denote the radiating SVWF reflected by the surface. For  $\mathbf{r}$  inside a sphere enclosed in the particle and a given azimuthal mode  $m$  the reflected SVWF are given by

$$\begin{pmatrix} \mathbf{M}_{mn}^{3,R}(k_0\mathbf{r}) \\ \mathbf{N}_{mn}^{3,R}(k_0\mathbf{r}) \end{pmatrix} = \sum_{n'=1}^{\infty} D_{mn'} \left[ \begin{pmatrix} \alpha_{mnn'} \\ \gamma_{mnn'} \end{pmatrix} \mathbf{M}_{mn'}^1(k_0\mathbf{r}) + \begin{pmatrix} \beta_{mnn'} \\ \delta_{mnn'} \end{pmatrix} \mathbf{N}_{mn'}^1(k_0\mathbf{r}) \right]. \quad (26)$$

Substituting (26) in (25) we get a representation of the interacting field in terms of regular SVWF, i.e.

$$\mathbf{E}_{\text{sca}}^R(\mathbf{r}) = \sum_{n'=1}^{\infty} \sum_{m=-n'}^{n'} D_{mn'} [e_{mn'}^R \mathbf{M}_{mn'}^1(k_0 \mathbf{r}) + f_{mn'}^R \mathbf{N}_{mn'}^1(k_0 \mathbf{r})], \quad (27)$$

where

$$\begin{pmatrix} e_{mn'}^R \\ f_{mn'}^R \end{pmatrix} = \sum_{n=1}^{\infty} D_{mn} \left[ \begin{pmatrix} \alpha_{mnn'} \\ \gamma_{mnn'} \end{pmatrix} e_{mn} + \begin{pmatrix} \beta_{mnn'} \\ \delta_{mnn'} \end{pmatrix} f_{mn} \right]. \quad (28)$$

In the extended boundary condition method the scattered field coefficients are related to the expansion coefficients of the fields striking the particle by the transition matrix. For an axisymmetric particle the equations become uncoupled, permitting a separate solution for each azimuthal mode. For a fixed azimuthal mode  $m$  we truncate the expansions given in (22), (24) and (27) and get the following matrix equation for the scattering problem

$$\begin{bmatrix} e_{mn} \\ f_{mn} \end{bmatrix} = [T_{mnn'}] \cdot \left( \begin{bmatrix} a_{mn'}^{\text{ref}} \\ b_{mn'}^{\text{ref}} \end{bmatrix} + \begin{bmatrix} e_{mn'}^R \\ f_{mn'}^R \end{bmatrix} \right). \quad (29)$$

Here,  $m = \overline{-M, M}$  and  $n, n' = \overline{1, N}$ , where  $M$  is the number of azimuthal modes and  $N$  is the truncation index. The expansion coefficients of the interacting field are related to the scattered field coefficients by a so called reflection matrix  $[A_{mnn'}]$ , that is

$$\begin{bmatrix} e_{mn'}^R \\ f_{mn'}^R \end{bmatrix} = [A_{mnn'}] \cdot \begin{bmatrix} e_{mn} \\ f_{mn} \end{bmatrix}. \quad (30)$$

The scattered field coefficients  $e_{mn}$  and  $f_{mn}$  are obtained by combining matrix equations (29) and (30). The explicit form of the reflection matrix can be found in [10,11].

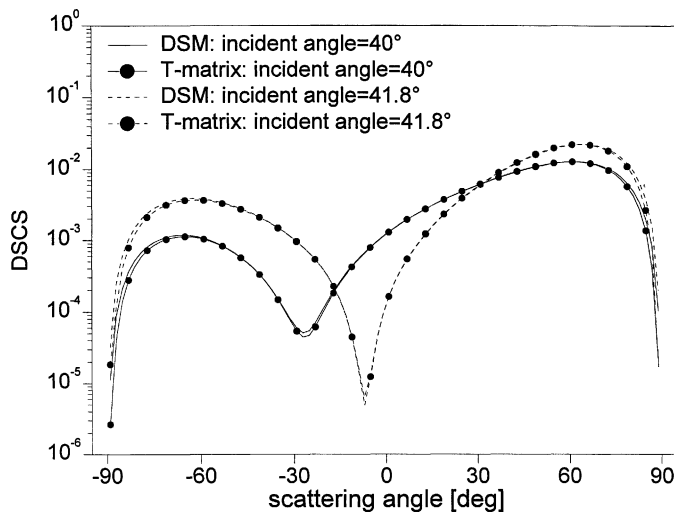


Fig. 2. Differential scattering cross section for a spherical particle with a diameter of  $d = 0.2 \mu\text{m}$  and a refractive index of  $n_i = 1.5$ . Two incident angles  $\beta_1 = 40^\circ$  and  $\beta_1 = 41.8^\circ$  are considered.

The main steps of the T-matrix approach are summarized as follows: calculation of the transition matrix which relates the expansion coefficients of the fields striking the particle to the scattered field coefficients; calculation of the reflection matrix characterizing the reflection of SVWF by the surface; computation of an approximate solution of the governing matrix equation, and extrapolation of the scattered field to the far field.

### 3. Numerical simulations

In this section we will investigate from a computational point of view the scattering of evanescent waves by particles deposited on a glass prism. The wavelength of the external excitation in free space is assumed to be  $\lambda_0 = 0.488 \mu\text{m}$ . The scatterer is deposited on a glass prism with a refractive index of  $n_1 = 1.5$ . The evanescent wave appears for incident angles  $\beta_1 > \beta_c$ , where  $\beta_c = 41.8^\circ$ . In Fig. 2 we plot the differential scattering cross

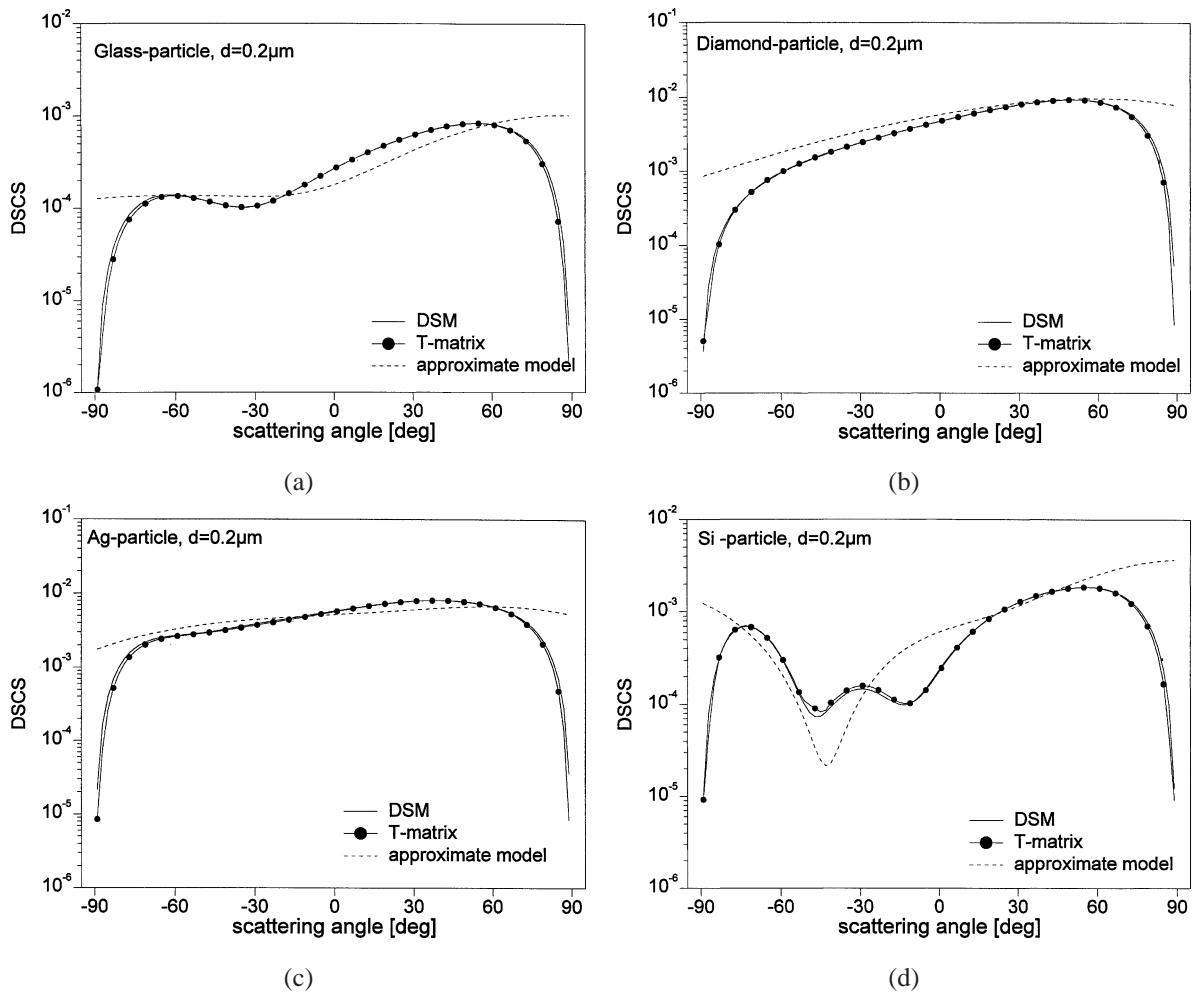


Fig. 3. Differential scattering cross section for spherical particles with a diameter of  $d = 0.2 \mu\text{m}$ . The curves correspond to (a) glass spheres ( $n_i = 1.5$ ), (b) diamond spheres ( $n_i = 2.43$ ), (c) metallic Ag-spheres ( $n_i = 0.25 + 3.14j$ ), and (d) Si-spheres ( $n_i = 4.37 + 0.08j$ ). The incident angle is  $\beta_1 = 60^\circ$ .

section for a spherical particle with a diameter of  $d = 0.2 \mu\text{m}$  and a refractive index of  $n_i = 1.5$  when the incident angle approaches to the critical value. It is readily seen that the changes in the scattering diagrams are pronounced in this domain. Note, that the curves are computed with the discrete sources method and the T-matrix method and no significant difference appears between the scattering characteristics.

As next we will investigate the accuracy of an approximate model for evanescent wave scattering. This model ignores the presence of the plane interface and has been used by Liu et al. [4] for analyzing the structural resonances in dielectric spheres illuminated by evanescent waves. In Fig. 3 we plot the differential scattering cross section for spherical particles of different materials with a diameter of  $d = 0.2 \mu\text{m}$ . The incident wave is a P-polarized plane wave and the scattering plane coincides with the incident plane. The angle of incidence is  $\beta_1 = 60^\circ$ . We examine the scattering by glass spheres ( $n_i = 1.5$ ), diamond spheres ( $n_i = 2.43$ ), metallic Ag-spheres ( $n_i = 0.25 + 3.14j$ ) and Si-spheres ( $n_i = 4.37 + 0.08j$ ). The plotted data show a good agreement between the exact models constructed on the basis of the discrete sources method and the T-matrix

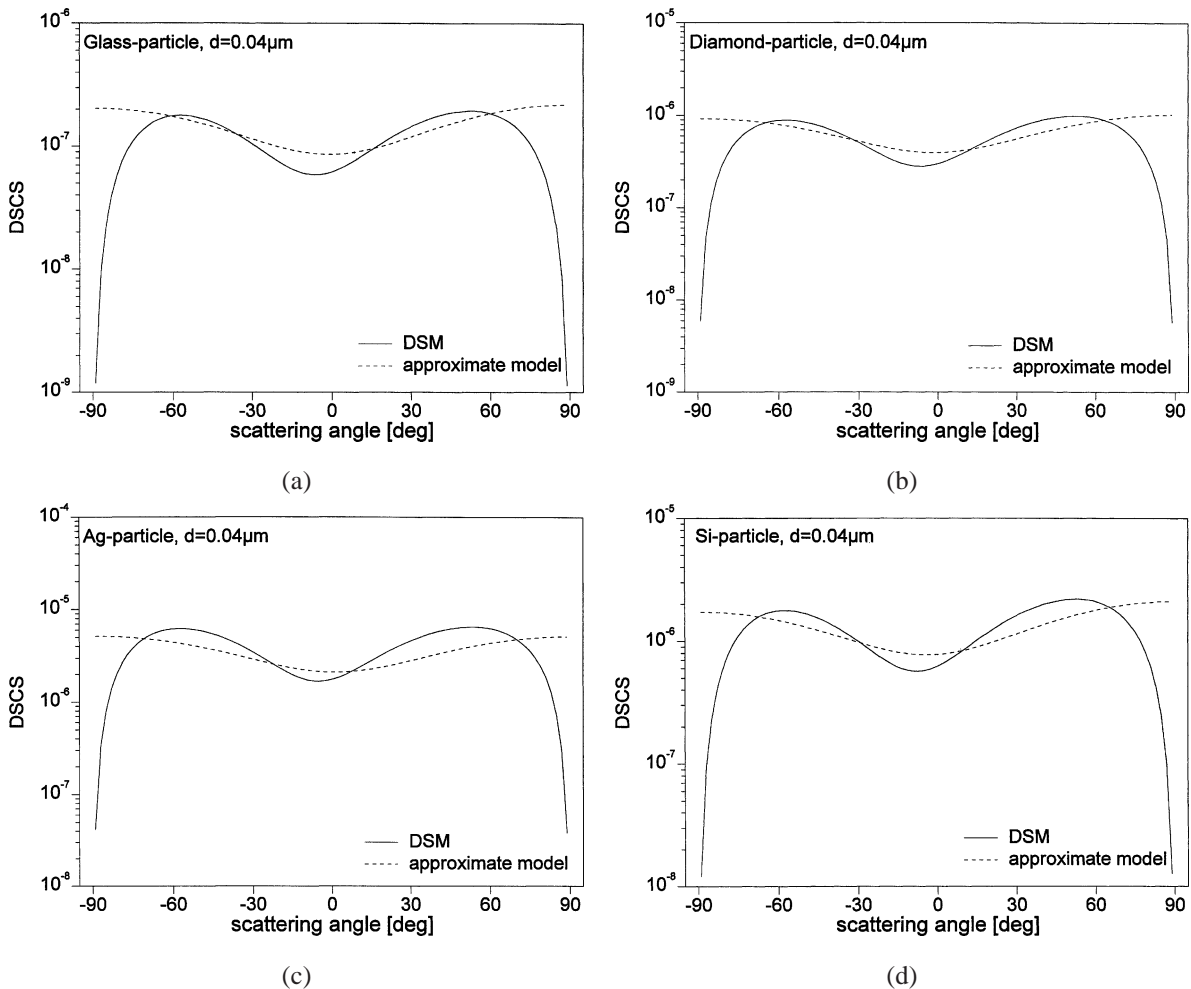


Fig. 4. Differential scattering cross section for spherical particles with a diameter of  $d = 0.04 \mu\text{m}$ . The curves correspond to (a) glass spheres ( $n_i = 1.5$ ), (b) diamond spheres ( $n_i = 2.43$ ), (c) metallic Ag-spheres ( $n_i = 0.25 + 3.14j$ ) and (d) Si-spheres ( $n_i = 4.37 + 0.08j$ ). The incident angle is  $\beta_1 = 60^\circ$ .

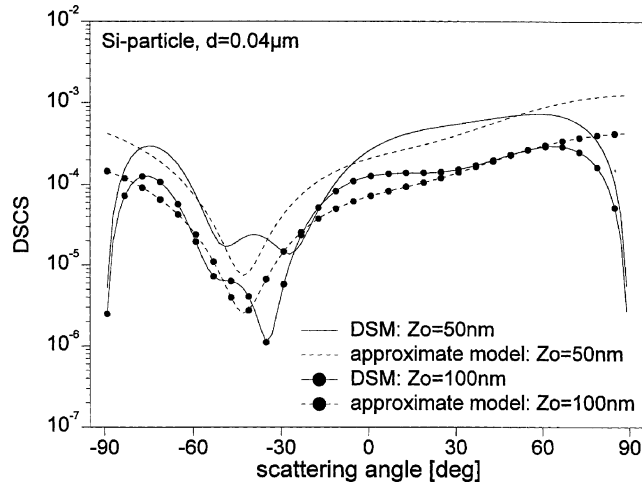


Fig. 5. Differential scattering cross section for a Si-sphere situated at different distances above the surface. The particle diameter is  $d = 0.2 \mu\text{m}$  and the incident angle is  $\beta_1 = 60^\circ$ .

method. In contrast, the approximate model leads to erroneous results. The main disagreement between the approximate and the exact models corresponds to the Si-sphere. This may be a consequence of the complex structure of the scattering diagram for Si-material. The same disagreement between the scattering curves can be observed for small spheres. In Fig. 4 we plot the differential scattering cross sections for spheres of different materials with a diameter of  $d = 0.04 \mu\text{m}$ . In this case the discrepancy is more pronounced for Ag-spheres.

In Fig. 5 we present computer results for a Si-sphere situated at different distances above the surface. The particle diameter is  $d = 0.2 \mu\text{m}$ . As expected, the errors between the scattering curves are significant when the distance between the particle and the plane surface decreases.

#### 4. Conclusion

Exact models for evanescent wave scattering has been constructed on the basis of the discrete sources method and the T-matrix method. In addition, the accuracy of an approximate model has been analyzed from a computational point of view. The computer results have shown a visible disagreement between the scattering curves, especially for particles with high index of refraction. Thus, we may conclude that only exact models describe adequately the scattering of evanescent waves by small particles.

#### Acknowledgements

This research was supported by DAAD (ref. 325, N A/99/09581).

#### References

- [1] R.C. Reddick, R.J. Warmack, T.L. Ferrell, New form of scanning optical microscopy, *Phys. Rev. B* 39 (1989) 767.
- [2] Y. Martin, F. Zenhausern, H.K. Wiskramasinghe, Scattering spectroscopy of molecules at nanometer resolution, *Appl. Phys. Lett.* 68 (1996) 2475.

- [3] R.C. Reddick, R.J. Warmack, D.W. Chilcott, S.L. Sharp, T.L. Ferrell, Photon scanning tunneling microscopy, *Rev. Sci. Instrum.* 61 (1990) 3669.
- [4] C. Liu, T. Kaiser, S. Lange, G. Schweiger, Structural resonances in a dielectric sphere illuminated by an evanescent wave, *Opt. Commun.* 117 (1995) 521.
- [5] P.C. Chaumet, A. Rahmani, F. Fornel, J.-P. Dufour, Evanescent light scattering: The validity of the dipole approximation, *Phys. Rev. B* 58 (1998) 2310.
- [6] M. Quinten, A. Pack, R. Wannemacher, Scattering and extinction of evanescent waves by small particles, *Appl. Phys. B* 68 (1999) 87.
- [7] R. Wannemacher, A. Pack, M. Quinten, Resonant absorption and scattering in evanescent fields, *Appl. Phys. B* 68 (1999) 225.
- [8] Yu.A. Eremin, N.V. Orlov, A.G. Sveshnikov, Models of electromagnetic scattering problems based on discrete sources methods, in: T. Wriedt (Ed.), *Generalized Multipole Techniques for Electromagnetic and Light Scattering*, Elsevier Science, Amsterdam, 1999, p. 39.
- [9] Yu.A. Eremin, N.V. Orlov, Simulation of light scattering from particle upon Wafer surface, *Appl. Opt.* 35 (1996) 6599.
- [10] T. Wriedt, A. Doicu, Light scattering from a particle on or a near a surface, *Opt. Commun.* 152 (1998) 376.
- [11] A. Doicu, Yu.A. Eremin, T. Wriedt, Convergence of T-matrix method for light scattering from a particle on or near a surface, *Opt. Commun.* 159 (1999) 266.